

ICSI 2019 The 3rd International Conference on Structural Integrity

# Fracture Resistance of Alkali Activated Concrete under the Mixed Mode I/II Load Conditions

Petr Miarka<sup>a,b,\*</sup>, Stanislav Seitl<sup>a,b</sup>, Oldřich Sucharda<sup>c</sup>, Vlastimil Bílek<sup>c</sup><sup>a</sup>*Faculty of Civil Engineering, Brno University of Technology, Veveří 331/95, Brno 602 00 Czech Republic*<sup>b</sup>*Institute of Physics of Materials of the Academy of Sciences of the Czech Republic, v.v.i., Žitkova 513/22, 616 62 Brno, Czech Republic,*<sup>c</sup>*Faculty of Civil Engineering, VSB-Technical University of Ostrava, L. Poděštné 1875/17, 708 33 Ostrava, Czech Republic*

---

## Abstract

Nowadays, traditional concrete mixture uses as a binder well known Portland cement. However, the production of the Portland cement is not environmentally friendly, due to high production of CO<sub>2</sub> in the fabrication process. In recent years, there are some trends to use secondary materials as a binder or as replacement of aggregate in the process of making the concrete mixture. This modified material uses alkali reaction in the hardening of fresh mixture, therefore an alkali activated concrete (AAC) term is used. This AAC is then used in formwork as it was traditional concrete, due to similar properties. Despite the use of advanced material, standards for structural design do not provide any instruction for practical application. Subsequently, the knowledge of fracture of this material is limited. The fracture mechanical properties help to perform advanced structural analysis, especially when some of the structural elements have a crack. The load presence on the structure can be divided into tensile, shear, and into combination of tension and shear. Therefore, it is necessary to perform test, which covers mixed mode I/II loading conditions. One of the tests usually used for the evaluation of fracture resistance of concrete is the Brazilian disc test with a central notch. This contribution evaluates the fracture resistance of alkali activated concrete, which will be used as a possible replacement for traditional structural concrete with cement binder, subjected to mixed mode I/II loading. The generalized maximum tangential stress (GMTS) criterion was used for the evaluation of the fracture resistance curve.

© 2019 The Authors. Published by Elsevier B.V.

Peer-review under responsibility of the ICSI 2019 organizers.

*Keywords:* Alkali activated material, Concrete, GMTS, MTS, Fracture mechanics.

---

\* Corresponding author. Tel.: +4-205-411-477-116.

*E-mail address:* petr.miarka@vut.cz

## Nomenclature

3PBT	Three-point bending test
BD	Brazilian disc
BDCN	Brazilian disc with a central notch
FMP	fracture mechanical parameter
SIF	Stress intensity factor
WST	Wedge-splitting test
$\alpha$	Crack inclination angle [°]
$\sigma_{\theta\theta}$	Tangential stress [MPa]
$\theta_0$	Crack initiation angle [°]
$a$	Notch length [mm]
$K_I, K_{II}$	Stress intensity factor for mode I and mode II [MPam <sup>1/2</sup> ]
$K_{IC}$	Fracture toughness [MPam <sup>1/2</sup> ]
$P$	Load [kN]
$P_C$	Fracture load [kN]
$R$	Radius [mm]
$r_C$	Critical distance [mm]
$T$	T-stress [MPa]

## 1. Introduction

To obtain a material sample from a structure to be renovated, a core-drill is used to remove a cylindrical sample from the structure, which is then submitted to a laboratory test to investigate the structure's material. Most of these laboratory tests investigate the mechanical behavior, while the fracture mechanical parameters (FMPs) are usually unintentionally omitted. Most of the common test specimens used in the evaluation of the FMPs have a rectangular shape with a square cross-section i.e. the WST by Tshegg (1991) or the 3PBT by RILEM (1985). To avoid expensive reshaping of core-drill samples into prisms, the use of the Brazilian disc specimen seems to be a good option.

In practice, two kinds of Brazilian disc tests are usually used. First, the unnotched Brazilian disc (BD) test is used to measure the indirect tensile strength  $f_t$  of rocks by Li and Wong (2013) and concrete in EN 12390-6 (2010), while the Brazilian disc with a central notch (BDCN) is used to evaluate fracture mechanical behavior (stress intensity factor (SIF) and fracture toughness  $K_{IC}$ ) by Ayatollahi and Aliha (2008). The BDCN test provides information of the SIF in tension (mode I), shear (mode II) and combination of tension and shear (mixed-mode I/II), hence it covers all possible loading cases present in the investigated structure. The measurement of the mixed mode I/II fracture parameters is done by inclining the initial notch against the load position by angle  $\alpha$  (See Fig. 1).

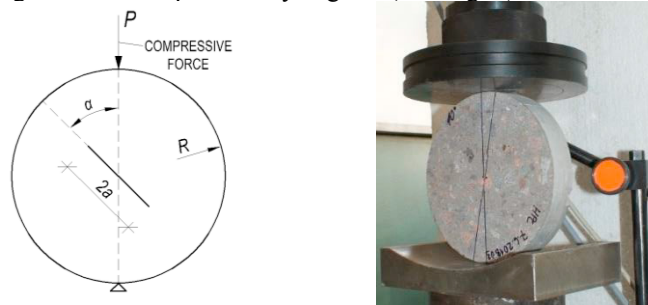


Fig. 1. Brazilian disc with central notch and applied boundary conditions (left) and experimental setup (right).

The main advantages of the BDCN test are that the tested specimens are usually thin (according the recommendation by Karihaloo (1995) five times max aggregates size, this means around 30 mm, compared to WST or 3PBT and the test is done under relatively simple experimental conditions (testing apparatus with sufficient capacity

is used). Based on this information, an assessment of fracture resistance of the investigated material can be done by analytical methods described in Ayatollahi and Aliha (2008).

In this contribution, the fracture resistance of two concrete types under the mixed mode I/II is compared. The selected materials can be characterized as a high-performance concrete, which are used in the production of precast concrete elements. The first concrete grade is standardly used in production of precast elements and it is referred as a C 50/60 see e.g. Seidl et al. (2018). The second concrete type is an alkali activated material, which uses secondary materials in the mixture composition. Therefore, this concrete is referred as an alkali activated concrete (AAC). The AAC has a compressive strength  $f_c$  comparable to C 50/60 MPa, therefore it should provide same structural behavior with less impact on the environment. The AAC should replace the C 50/60 concrete and allow to produce structural elements, which should lead to a reduction of production expenses, due to no cement presence in the mixture. The fracture resistance under mixed mode I/II is analyzed by employing the maximum tangential stress (MTS) criterion proposed by Erdogan and Sih (1963) and the generalized maximum tangential stress (GMTS) criterion proposed by Smith et al. (2001). The discussion on the accurate selection of critical distance  $r_c$  is present for both studied concrete types.

## 2. Theoretical Background

This contribution is based on linear elastic fracture mechanics (LEFM). The LEFM concept uses the stress field in the close vicinity of the crack tip described by the expansion proposed by Williams (1956). This expansion is an infinite power series originally derived for a homogenous elastic isotropic cracked body, which can be described by the following equation:

$$\sigma_{i,j} = \frac{K_I}{\sqrt{2\pi r}} f_{i,j}^I(\theta) + \frac{K_{II}}{\sqrt{2\pi r}} f_{i,j}^{II}(\theta) + T + O_{i,j}(r, \theta), \quad (1)$$

where  $\sigma_{ij}$  represents the stress tensor components.  $K_I$ ,  $K_{II}$  are the SIFs for mode I and respectively mode II,  $f_{i,j}^I(\theta)$ ,  $f_{i,j}^{II}(\theta)$ , are known shape functions for mode I and mode II usually written as  $Y_I$  and  $Y_{II}$ ,  $T$  (or T-stress) represents the second independent term on  $r$ .  $O_{ij}$  represents higher order terms and  $r$ ,  $\theta$  are polar coordinates (with origin at the crack tip; the crack faces lie along the x-axis).

The SIF values for a finite specimen and a polar angle  $\theta = 0^\circ$  can be expressed in the following from Tada et al. (2000) or Anderson (2017):

$$K_I = \frac{P\sqrt{a}}{RB\sqrt{\pi}} \frac{1}{\sqrt{1-\frac{a}{R}}} Y_I\left(\frac{a}{R}, \alpha\right) \quad (2)$$

$$K_{II} = \frac{P\sqrt{a}}{RB\sqrt{\pi}} \frac{1}{\sqrt{1-\frac{a}{R}}} Y_{II}\left(\frac{a}{R}, \alpha\right). \quad (3)$$

The values of the T-stress for the BDCN geometry can be found in literature, i.e. Ayatollahi and Aliha (2008) and Seidl et al. (2018) or calculated using a direct extrapolation method proposed by Yang and Ravi-Chandar (1999) as:

$$T = \lim_{r \rightarrow 0} (\sigma_{xx} - \sigma_{yy}). \quad (4)$$

### 2.1. Fracture Criteria for Mixed mode I/II

Based on the knowledge of geometry functions, SIFs and T-stress, the tangential stress  $\sigma_{\theta\theta}$  from the Eq. 1 can be formulated as:

$$\sigma_{\theta\theta} = \frac{1}{\sqrt{2\pi r}} \cos \frac{\theta}{2} \left[ K_I \cos^2 \frac{\theta}{2} - \frac{3}{2} K_{II} \sin \theta \right] + T \sin^2 \theta + O(r^{1/2}). \quad (5)$$

To determinate the onset of fracture under the mixed mode I/II loading conditions, the MTS and GMTS criteria are used. Both criteria can be evaluated from:

$$\frac{\partial \sigma_{\theta\theta}}{\partial \theta} |_{\theta=\theta_0} = 0 \text{ and } \frac{\partial^2 \sigma_{\theta\theta}}{\partial^2 \theta} < 0. \quad (6)$$

## 2.2. Maximum Tangential Stress Criterion

According to the assumption of MTS criterion from Eq. 6, the angle of maximum tangential stress  $\theta_0$  is determined from:

$$[K_I \sin \theta_0 + K_{II}(3 \cos \theta_0 - 1)] = 0. \quad (7)$$

In this case, the angle  $\theta_0$  depends only on mode I and mode II SIFs ( $K_I$  and  $K_{II}$ ) and it is used in the prediction of fracture resistance under the mixed mode I/II.

## 2.3. Generalized Maximum Tangential Stress Criterion

While the MTS criterion uses only SIFs for the determination of the crack initiation angle  $\theta_0$ , the GMTS uses two more parameters i.e. the T-stress and the critical distance  $r_C$ . The angle  $\theta_0$  can be calculated from Eq. 6, which leads in case of GMTS into:

$$[K_I \sin \theta_0 + K_{II}(3 \cos \theta_0 - 1)] - = 0. \quad (8)$$

As it can be noticed from Eq. 8, the GMTS depends also on  $K_I$ ,  $K_{II}$ , T-stress and the critical distance  $r_C$  (if  $r_C = 0$  GMTS leads to MTS). Thus, the selection of the critical distance plays a key role in the evaluation of the fracture resistance under the mixed mode I/II loading. The literature Anderson (2017) and Seitzl et al. (2018) proposes several methods for calculation of critical distance based on the boundary conditions, see Eqs. 9-10.

$$r_C = \frac{1}{2\pi} \left( \frac{K_{IC}}{\sigma_t} \right)^2, \text{ - plane stress} \quad (9)$$

$$r_C = \frac{1}{6\pi} \left( \frac{K_{IC}}{\sigma_t} \right)^2 \text{ - plane strain} \quad (10)$$

The onset of fracture occurs when the  $\sigma_{\theta\theta}$  reaches its critical value  $\sigma_{\theta\theta,C}$ . This critical value is reached when  $\sqrt{2\pi r_C} \sigma_{\theta\theta,C} = K_{IC}$ , i.e. the material fracture toughness is reached. This assumption is then substituted to Eq. 5 and the fracture resistance curve under the mixed mode I/II can be obtained from:

$$K_{IC} = \cos \frac{\theta_0}{2} \left[ K_I \cos^2 \frac{\theta_0}{2} - \frac{3}{2} K_{II} \sin \theta_0 \right] + \sqrt{2\pi r_C} T \sin^2 \theta_0. \quad (11)$$

## 3. Materials

The C 50/60 concrete type was chosen for this study because it is typically used in the production of pre-stressed precast elements. C 50/60 has a variety of structural applications because of its high compressive and tensile strength. However, this concrete type is characterized by a high cement content, which increases production expenses and has a high impact on the environment. Therefore, the producer of precast structural elements decided to change its production to be more environmentally friendly. These demands lead into development of a new concrete mixture, which uses secondary materials as a binder and has similar mechanical properties as C 50/60 concrete type with same structural response to the loading. The detailed mixture composition of the C 50/60 and the ACC are described below.

### 3.1. C 50/60

The C 50/60 concrete contains 450 kg of CEM I 42.5 R, and the water to cement ratio  $w/c$  is 0.40. The fine aggregate was natural sand 0/4 mm and crushed aggregates from 4/8 to 8/16 mm from high quality granite. The concrete was mixed in a volume of 1 m<sup>3</sup> and immediately poured into molds. A polycarboxylates-based superplasticizer was used to reach good workability. For more details see Seitl et al. (2018)

### 3.2. Alkali activated concrete

Alkali activated concrete (AAC) was designed based on formerly performed tests, see e.g. Bílek et al. (2010). The mixture composition is shown in Table 1. The dry mass of activator was 8 % and the water to slag ratio was 0.45. Sodium water glass and potassium hydroxide were combined to reduce efflorescence, see Szklorzová and Bílek (2008) and an appropriate silicate modulus of activator ( $M_s = 0.67$  or mass ratio  $(K_2O + Na_2O) / SiO_2$  is 60/40). This composition of activator is convenient in terms of both setting and strengths. Naphthalene based plasticizer was also used for better workability of the mixture.

Table 1: Mixture composition of alkali activated concrete.

	GBFS	Na-WG Ms = 2.0	50 % solution of KOH	water	PSN- plasticizer	Sand 0/4 mm	Crushed aggregates 4/8 mm	Crushed aggregates 8/16 mm
[kg/m <sup>3</sup> ]	450	45	34	159	10	855	385	400

### 3.3. Mechanical properties

To test the mechanical properties, 150 mm cubes and 150 mm diameter and 300 mm height cylinders were prepared - see Table 2. All the specimens were carefully enveloped with PE-foil (to prevent moisture exchange with the environment) and stored outside the laboratory (temperature  $\approx 5 - 25^\circ\text{C}$  for 28 days). The measured values are in accordance of European standards (EN 12390).

Table 2: Comparison of mechanical properties with standard deviation of studied concrete types in 28 days.

	C 50/60	AAC
Compressive cube strength $f_{c,cube}$ [MPa]	$85.8 \pm 2.9$	$62.0 \pm 1.5$
Compressive cylindrical strength $f_{c,cyl}$ [MPa]	$72.8 \pm 2.5$	$48.0 \pm 3.4$
Indirect tensile strength $f_t$ [MPa]	$5.52 \pm 0.31$	$3.153 \pm 0.18$
Young's Modulus $E$ [GPa]	$38.3 \pm 0.3$	$26.3 \pm 1.1$
Bulk density $\rho$ [kg/m <sup>3</sup> ]	$2390.0 \pm 27.32$	$2245.0 \pm 14.58$

## 4. Mixed mode I/II Experimental Results

As this contribution focuses on the fracture resistance of mixed mode I/II, firstly the measured experimental fracture forces  $P_C$  and equivalent of SIFs values are shown. Afterwards, the evaluation of the MTS and GMTS is present. The fracture resistance curves for both materials are compared for same boundary conditions.

The specimens had the radius  $R$  of 75 mm, the thickness  $B$  of 30 mm (there is only a relatively small discrepancy between them). In total, two relative notch lengths  $2a$  were tested. First notch length was  $2a = 40$  mm and the second one  $2a = 60$  mm, which in terms of relative notch lengths gives ratio  $a/R = 0.267$  and 0.4. SIF values were evaluated using Eqs. 2 and 3. This was done for mode I (inclination angle  $\alpha = 0^\circ$ ), for mode II (inclination angle  $\alpha = 27.2^\circ$ ) and for mixed mode I/II (for any other angle  $\alpha$ ). More specifically, the notch inclination angles  $\alpha$  were for  $a/R = 0.267$   $\langle 0^\circ; 5^\circ; 10^\circ; 15^\circ; 20^\circ; 27.7^\circ \rangle$  and for  $a/R = 0.4$   $\langle 0^\circ; 5^\circ; 10^\circ; 15^\circ; 20^\circ; 25.2^\circ \rangle$ . Measured/obtained maximum loads are summed up in Fig. 2.

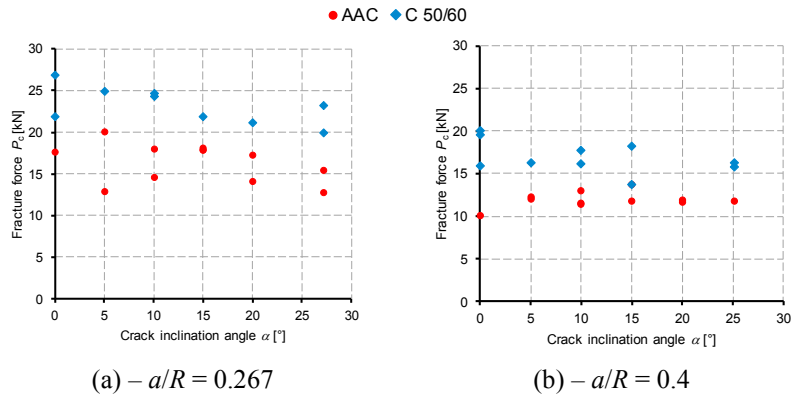


Fig. 2. Fracture loads  $P_C$  for selected angles  $\alpha$  in case of relative notch length  $a/R=0.267$  (a) – C 50/60 and (b) – AAC

The FMPs evaluated from the BDCN tests are presented below. In order to evaluate the fracture resistance curve, a fracture toughness  $K_{IC}$  was measured on BDCN for  $\alpha = 0^\circ$  for which a critical distance  $r_c$  was evaluated according to Eqs. 9 and 10. These values are presented in

Table 3 for both studied concrete mixtures.

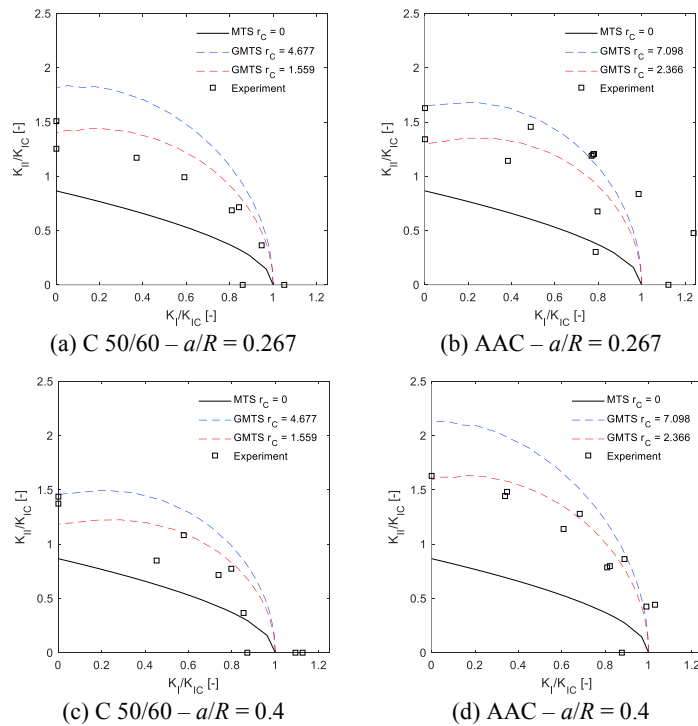


Fig. 3. Comparison of evaluated fracture resistance curves for relative notch lengths  $a/R = 0.267$  and  $0.4$  for both studied materials C 50/60 and AAC.

Table 3: Comparison of fracture toughness  $K_{IC}$  measured on BDCN specimen and critical distances  $r_C$  for both studied materials C 50/60 and AAC.

Material	C 50/60			AAC		
Relative notch length $a/R$ [-]	0.267	0.400	Average	0.267	0.400	Average
$K_{IC} - BDCN [MPa\sqrt{m}]$	0.903	0.973	0.945	0.748	0.584	0.665
$r_C - plane\ stress [mm]$	4.271	4.958	4.677	8.953	5.457	7.098
$r_C - plane\ strain [mm]$	1.423	1.653	1.559	2.984	1.819	2.366

Firstly, the FMPs ( $K_I$  and  $K_{II}$ ) were evaluated using the fracture forces  $P_C$  presented in Fig. 2 and by employing the Eqs. 2-3. Afterwards, MTS and GMTS criteria have been employed for various  $a/R$  ratios and for various critical distances  $r_C$ . In the evaluation of fracture resistance, average values of both  $K_{IC}$  and  $r_C$  have been used, due to the lack of experimental data for AAC material for pure mode I. The evaluated fracture resistance curves of mixed mode I/II are presented in Fig. 3.

From Fig. 3, it can be noted that the selection of critical distance  $r_C$  has a major influence on the shape of fracture resistance curve. The MTS criterion is very conservative and does not predict the fracture resistance with good agreement. Nevertheless, the GMTS shows relatively good prediction of fracture under the mixed mode I/II for AAC material. From Fig. 3(b) and Fig. 3(d) a good agreement is observable for plane strain boundary conditions ( $r_C = 2.366$  mm). Similar assessment can be made for the C 50/60 material i.e. the plane strain boundary conditions case ( $r_C = 1.559$  mm) predicts the fracture resistance with a more reasonable agreement.

A comparison was drawn amongst both materials and studied boundary conditions as shown in Fig. 4. From which, a relatively small difference in prediction of mixed mode I/II fracture between C 50/60 and AAC can be inferred. This could be improved by selecting different value of critical distance or by providing more experimental measurements.

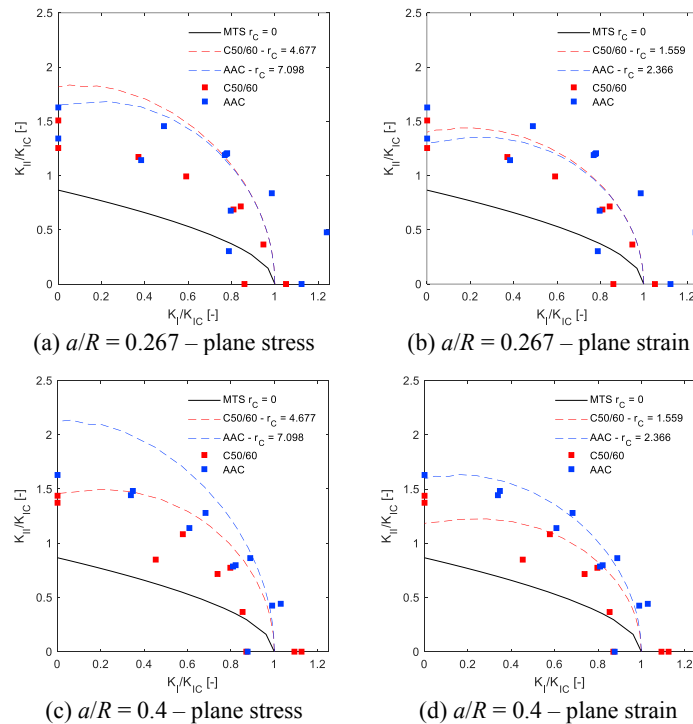


Fig. 4. Comparison of fracture resistance curve of C 50/60 and AAC material for various boundary conditions and its influence on the shape of the fracture resistance curve.

## Conclusion

From presented experimental results, following conclusion can be made:

- The selection of the critical distance  $r_c$  has a major influence on the good fitting of fracture resistance curve for given type of material.
- It was shown, that the value of  $r_c$  for plane strain boundary conditions shows relatively good prediction of fracture behavior for both types of concrete under the mixed mode I/II.
- In general, the AAC material has a better fracture resistance than the C 50/60 material. This is correlation with values for tensile and compressive strengths of C 50/60 in comparison with AAC material (concrete with high compressive strength show more brittle behavior).

## Acknowledgement

The research is partially supported by MEYS: projects FAST-J-19-5783 and by the Czech Science Foundation: project GJ18-12289Y and by project of conceptual research VSB -TU Ostrava. The first author is Brno Ph.D. Talent Scholarship Holder – Funded by the Brno City Municipality.

## References

- E. Tschegg, New Equipments for Fracture Tests on Concrete, *Material Testing* 33 (1991) 338–342
- Rilem, Recommendation, Determination of the fracture energy of mortar and concrete by means of three-point bend tests on notched beams, *Mat. and struct.*, 18 (1985) 285–290.
- D. Li, L.N.Y. Wong, The Brazilian disc test for rock mechanics applications: Review and new insights, *Rock Mech. and R. Eng.*, 46 (2013) 269–287.
- EN 12390-6: Testing hardened concrete. Tensile splitting strength of test specimens, 2010.
- M.R. Ayatollahi, M.R.M. Aliha, On the use of Brazilian disc specimen for calculating mixed mode I-II fracture toughness of rock materials, *Eng. Frac. Mech.*, 75 (2008) 4631–4641.
- T.L. Anderson, *Fracture mechanics: fundamentals and applications*, CRC press, 2017.
- M.L. Williams, On the Stress Distribution at the Base of a Stationary Crack, *J. of App. Mech.* 24 (1956).
- B. Yang, K. Ravi-Chandar, Evaluation of elastic T-stress by the stress difference method, *Engineering Fracture Mechanics*, 64 (1999) 589–605.
- F. Erdogan, G.C. Sih, On the Crack Extension in Plates Under Plane Loading and Transverse Shear, *Journal of Basic Engineering*, Vol. 85 (1963) 519–525.
- D.J. Smith, M.R. Ayatollahi, M.J. Pavier, The role of T-stress in brittle fracture for linear elastic materials under mixed-mode loading, *Fat. & Frac. of E. Mat. & Struct.* 24 (2001) 137–150.
- European Committee for Standardization, EN 12390-3: Testing hardened concrete, in: Part 3: Compressive strength of test specimens, 2009.
- European Committee for Standardization, EN 12390-5: Testing hardened concrete in: Part 5: Flexural strength of test specimens, 2009.
- International Organization for Standardization, Testing of concrete in: Part 10: Determination of static modulus of elasticity in compression, 2010.
- S. Seidl, P. Miarka, V. Bílek, The Mixed-Mode Fracture Resistance of C 50/60 and its Suitability for Use in Precast Elements as Determined by the Brazilian Disc Test and Three-Point Bending Specimens. *Theo. and App. Fract. Mech.* 97 (2018) 108–119.
- P. Miarka, S. Seidl, V. Bílek, Mixed-mode fracture analysis in High-performance concrete using Brazilian disc test. *Mat. & Tech.*, 53(2) (2019) 233–238.
- B. L. Karihaloo, P. Nallathambi, Effective crack model for the determination of fracture toughness (K<sub>ICe</sub>) of concrete. *Eng. Fract. Mech.*, 35 (1990), 4–5, 637–645.
- B. L. Karihaloo, *Fracture mechanics and structural concrete* Longman Pub Group (July 1, 1995), p. 330, ISBN: 978-0582215825
- H. Tada, P.C. Paris, G.R. Irwin, *The stress analysis of cracks handbook*, 3rd ed., ASME Press ASM International, New York, 2000.
- Bílek V., Opravil, T., Soukal, F., 2010. Searching for practically applicable alkali-activated concretes. 1st Int. Conf. on Advances in Chemically-Activated Materials 28–35.
- Szklorzová, H., Bílek, V., 2008. Influence of alkali ions in the activator on the performance of alkali activated mortars. *Proc. of 3rd International Symposium Non-Traditional Cement and Concrete*, 777 – 784.
- Sucharda, O., Bílek, V., Mateckova, P., Pazdera, L. 2018. AAM for Structure Beams and Analysis of Beam without Shear Reinforcement. *Solid State Phenomena*, 292:3–8,